ICME for Creep of Ni-Base Superalloys in Advanced Ultra-Supercritical Steam Turbines

Pengyang Zhao[1], **Supriyo Chakraborty**[1], **Mengfei Yuan**[1]

Yunzhi Wang[1], **and Stephen Niezgoda**[1,2]

[1]Department of Materials Science and Engineering, The Ohio State University

[2]Department of Mechanical and Aerospace Engineering, The Ohio State University

Acknowledgement

Bryce Meredig (Citrine Informatics)

Chen Shen (GE-GRC)

NATIONAL ENERGY TECHNOLOGY LABORATORY

(DE-FE0027776)

2018 NETL Annual Review Meeting for Crosscutting Research

Apr. 10-12, Pittsburgh, PA

Large Data Scatter for Creep Performance

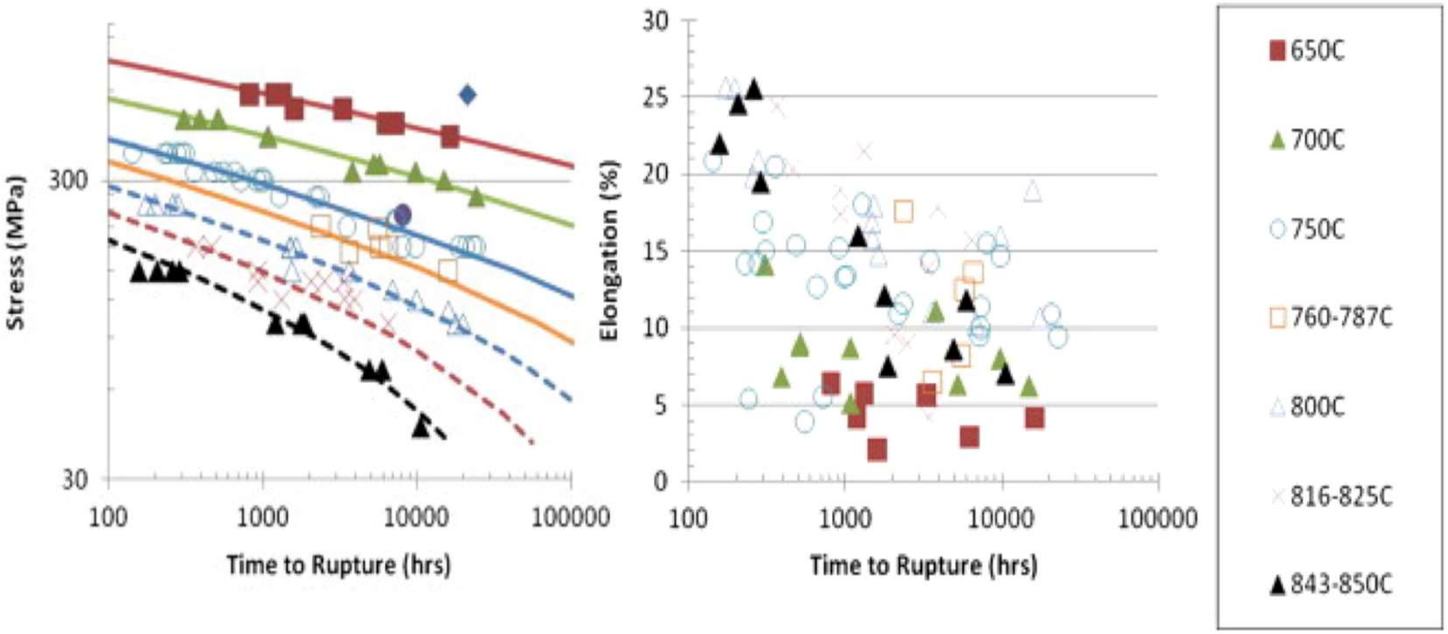

Rupture time vs. Stress/Elongation at various temperatures for Inconel 740 (Shingledecker, et. al, 2013)

- **The scatter is primarily due to material variability at the microstructure level**
- **Microstructure variability -> Data analysis & creep model.**

Current Creep Modeling of Ni-base Superalloys

Larson-Miller parameter (LMP) vs stress for various Ni-base superalloys ($C_{LM} = 20$)

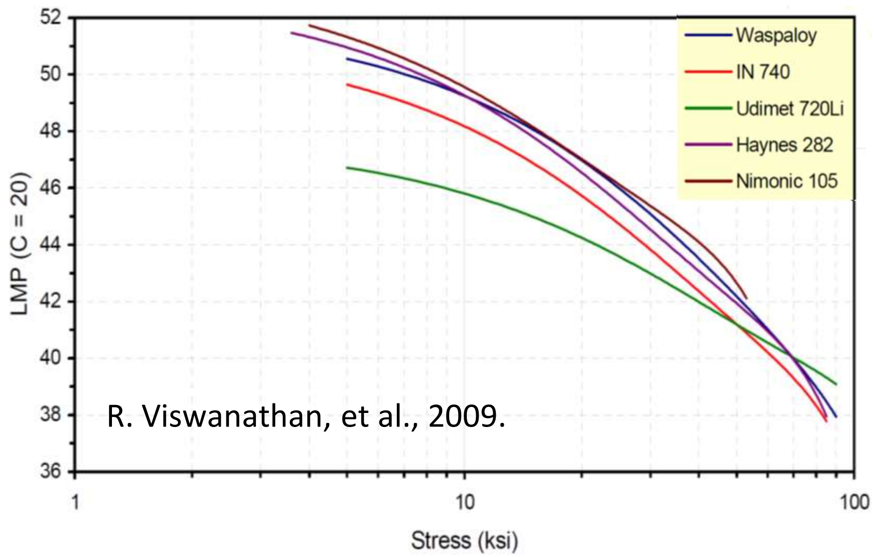

Rupture time

$$T[C_{LM} + \log t_r] = LMP = f(\sigma)$$

LM constant

- **Phenomenological in nature: simple analytical model by directly linking test conditions (e.g., stress) with creep measures (e.g., rupture time)**
- **No microstructure information is considered (The Larson-Miller constant is insensitive to the microstructure)**
- **No creep mechanisms are involved**
- **Cannot provide feedback on optimization of improving Ni-base superalloys**
- **Rely on sufficiently large amount of data (not efficient)**

Program Objectives

1. Application of advanced materials informatics for critical assessment of existing experimental data

2. Critical assessment of existing modeling capabilities

3. Development of new modeling capabilities that are critical but currently missing in predicting long-term creep behavior of Ni-base superalloys

Outline

- **Application of machine learning methods for prediction of structure-property relationships in Ni-base superalloys.**

  A fast-acting, reduced-order, data-driven tool

- **Development of a multiscale physics-based creep model for Ni-base superalloys**

  Integrated creep model at single crystal level

  Homogenized creep model at polycrystal level

Outline

- **Application of machine learning methods for prediction of structure-property relationships in Ni-base superalloys.**
  - A fast-acting, reduced-order, data-driven tool

- **Development of a multiscale physics-based creep model for Ni-base superalloys**
  - Integrated creep model at single crystal level
  - Homogenized creep model at polycrystal level

Machine Learning

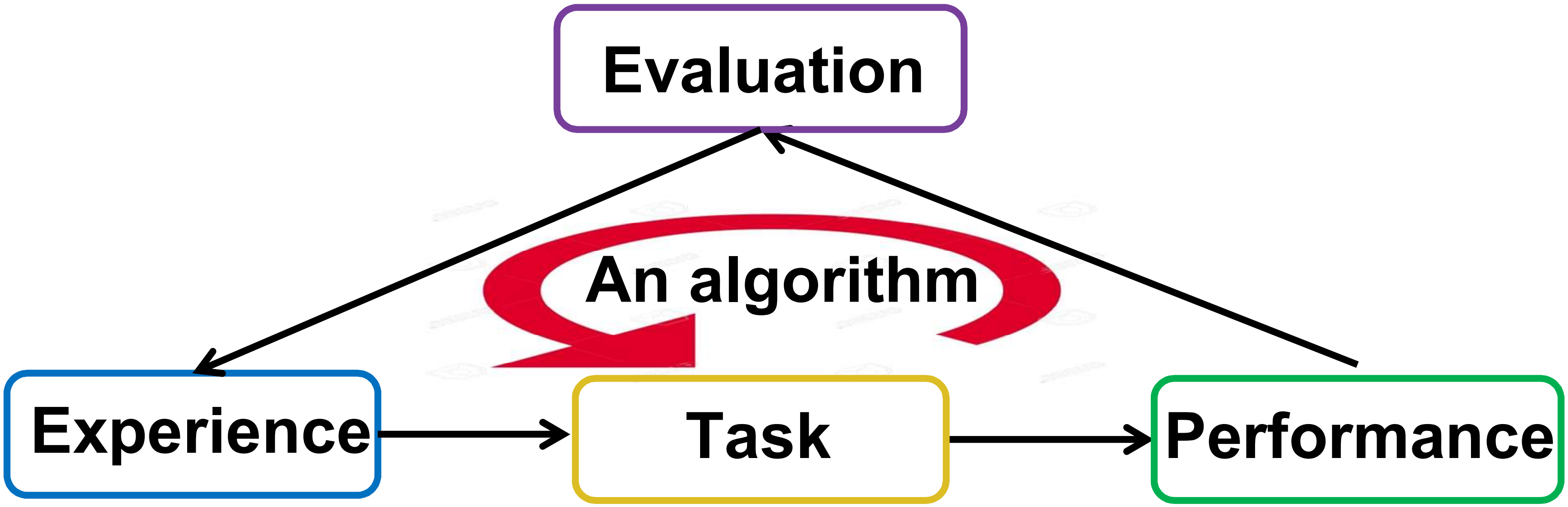

What's so special about ML?

- Algorithms *built on experience* (data) rather than specific instructions of how tasks should be done.
- *Tunable parameters* that are adjusted automatically to improve the performance by adapting to previously seen data.

ML Application to Materials Science

Data

- Size
- Representation
- Uncertainty

Challenge!

Algorithm ← **ML community**

Practice → Predictive model useful in materials applications

ML Application to Materials Science

	Example Methods	Selected Materials Applications
Supervised learning	Regularized least squares Support vector machines Kernel ridge regression Neural networks Decision trees Genetic programming	Predict processing structure–property relationships; develop model Hamiltonians; predict crystal structures; classify crystal structures; identify descriptors
Unsupervised learning	*k*-Means clustering Mean shift theory Markov random fields Hierarchical cluster analysis Principal component analysis Cross-correlation	Analyze composition spreads from combinatorial experiments; analyze micrographs; identify descriptors; noise reduction in data sets

(Mueller, et. al, 2016)

The data challenge is currently addressed mainly by utilizing computational data

A ML Approach to Structure-Property Relations

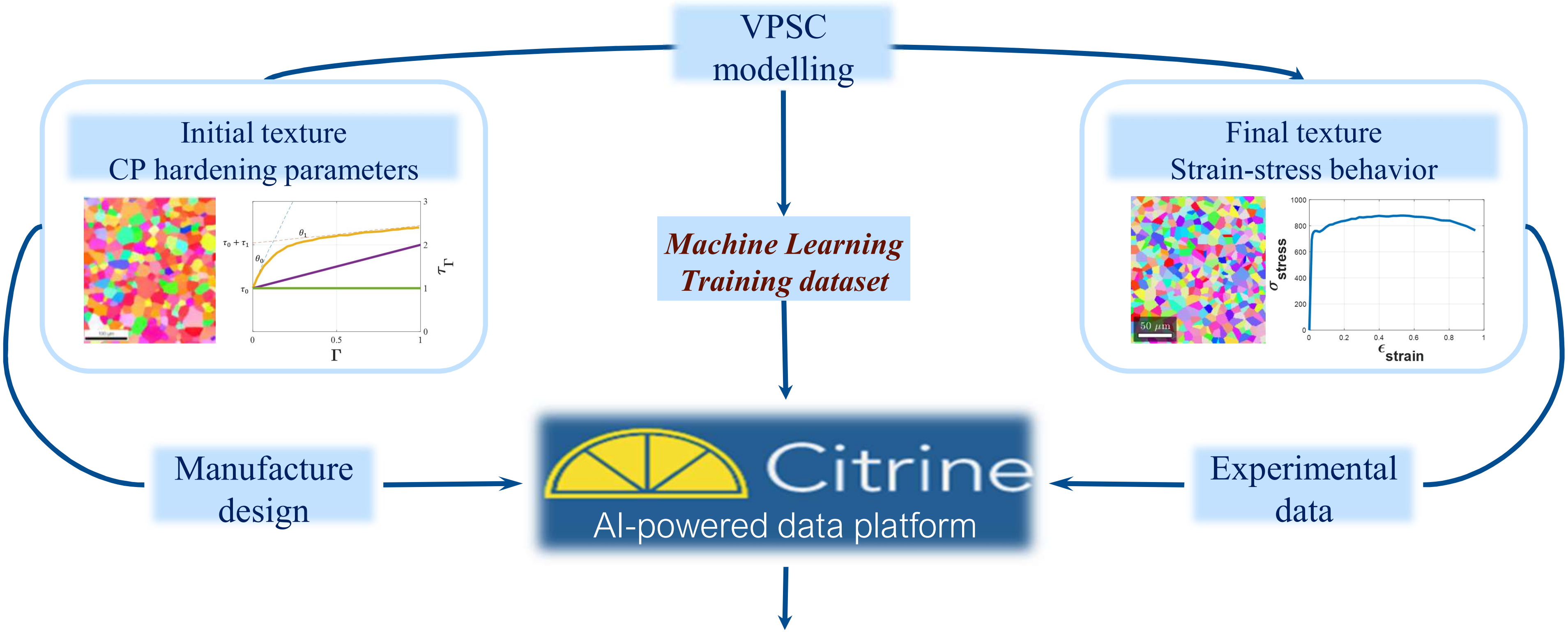

Goal: Fast-acting reduced-order data-driven tool

Invertible pathway: processing – microstructure – property/performance

Data Generation using VPSC Model

Build comprehensive training data using VPSC modeling determination:

Processing, velocity gradient, strain rate, sensitivity rate, grain interactions, boundary condition, crystal system, slip/twining mode, temperature, etc

Categories	Number	Boundary conditions
Loading condition	4	Uniaxial compression/Tension/ Simple shear / Rolling
Normalized Voce hardening parameters	10	$\frac{\tau_1^s}{\tau_0^s} = [\,0{:}\,1];\quad \frac{\theta_0^s}{\tau_0^s} = [\,0{:}\,5];\quad \frac{\theta_1^s}{\tau_0^s} = [\,0{:}\,2];$ Randomly generate using Latin-hyper cube sampling
Initial texture	12*5=60	12 standard texture created by MTEX; Cube, Goss, brass, Copper, S1, S2, S3, Taylor, uniform, alpha fiber, beta fiber, tau fiber; Randomly choose 5 examples from each category;
Velocity Gradient	4	[1, 0.1, 0.001, 0.0001]

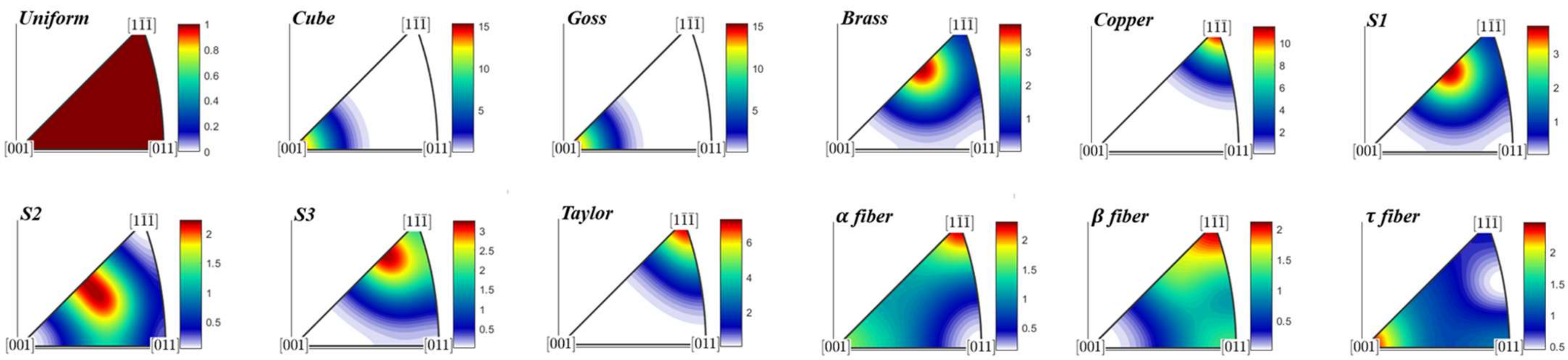

Property Prediction using the ML tool

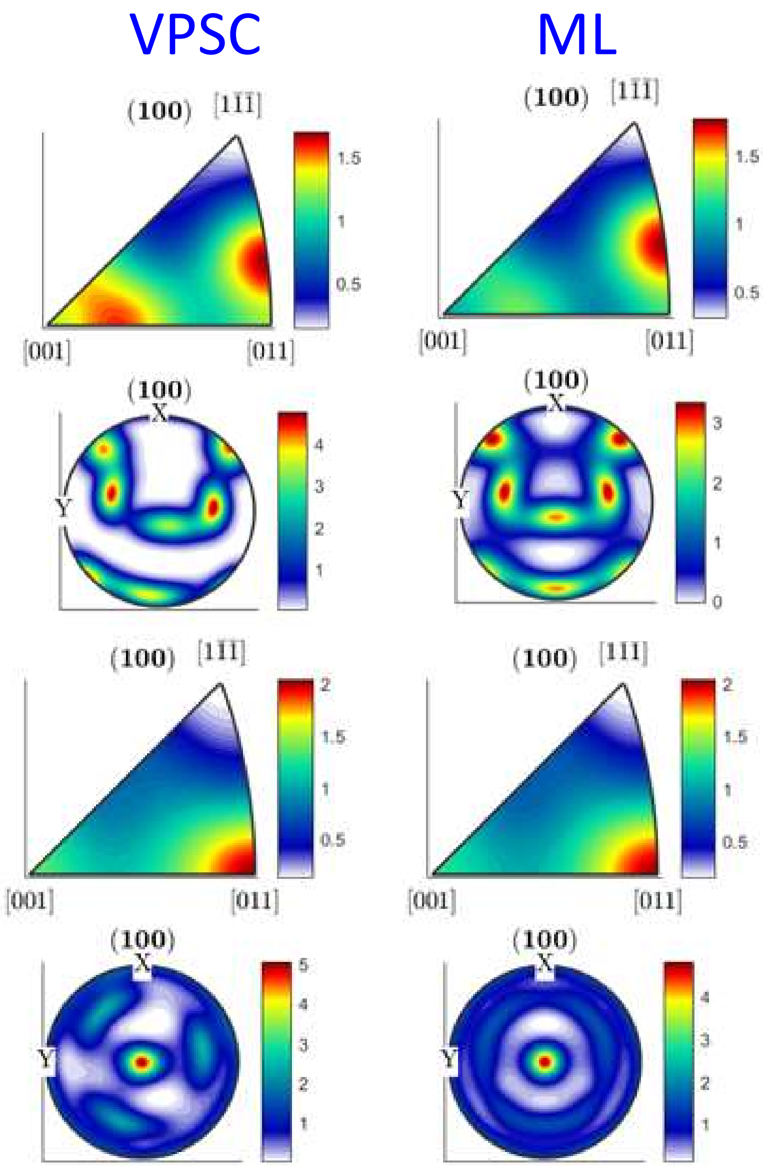

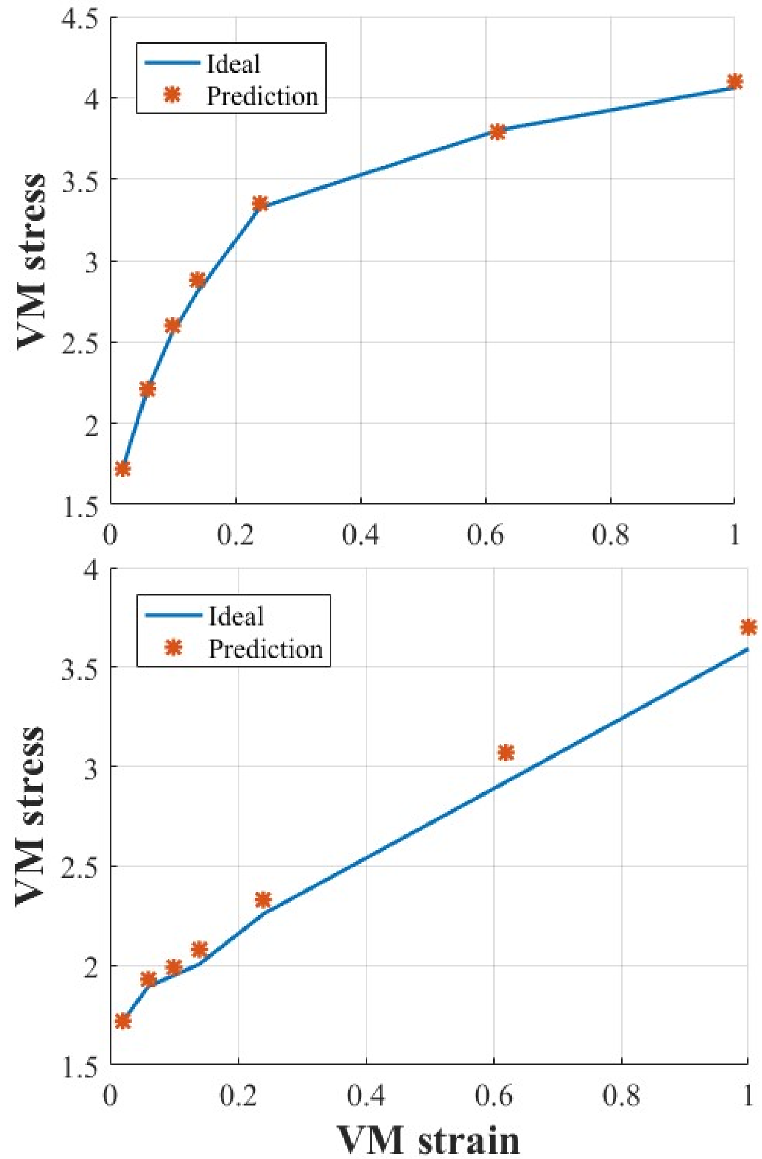

Calibration of the Proposed ML tool

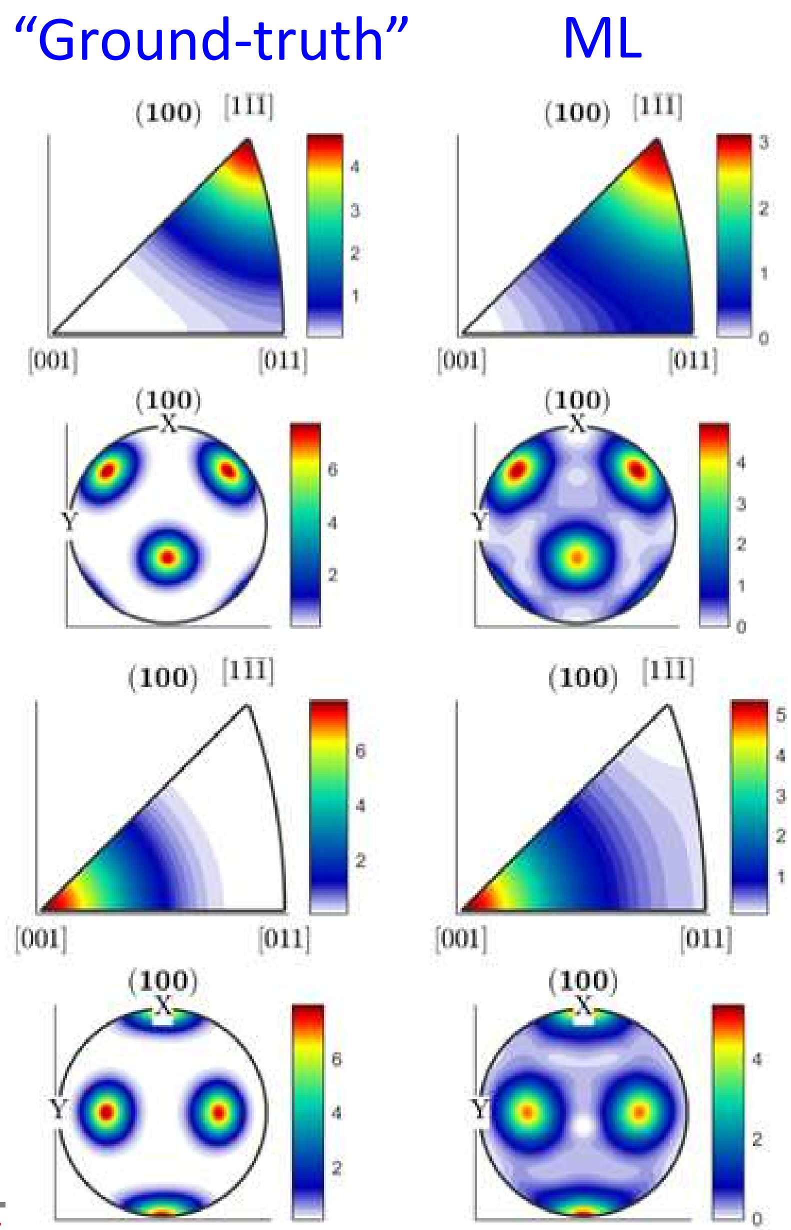

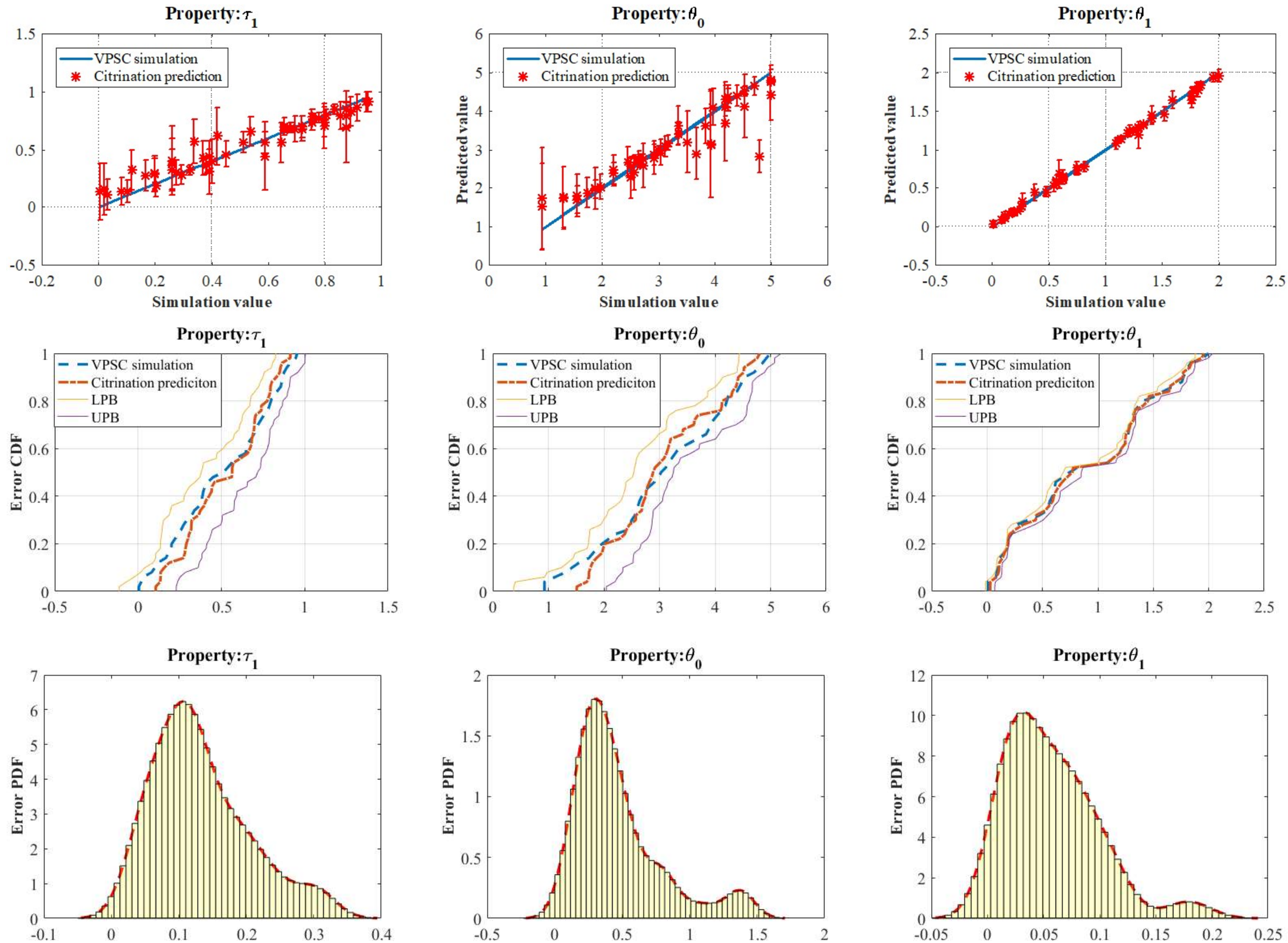
Property: τ_1
Property: θ_0
Property: θ_1
VPSC simulation
Citrination prediction
Predicted value
Simulation value
Error CDF
Citrination prediciton
LPB
UPB
Error PDF
UNIVERSITY

Outline

- Application of machine learning methods for prediction of structure-property relationships in Ni-base superalloys.

  A fast-acting, reduced-order, data-driven tool

- **Development of a multiscale physics-based creep model for Ni-base superalloys**

  Integrated creep model at single crystal level

  Homogenized creep model at polycrystal level

An Integrated Modeling Scheme

Multiscale, Microstructure-Sensitive, Mechanism-Informed

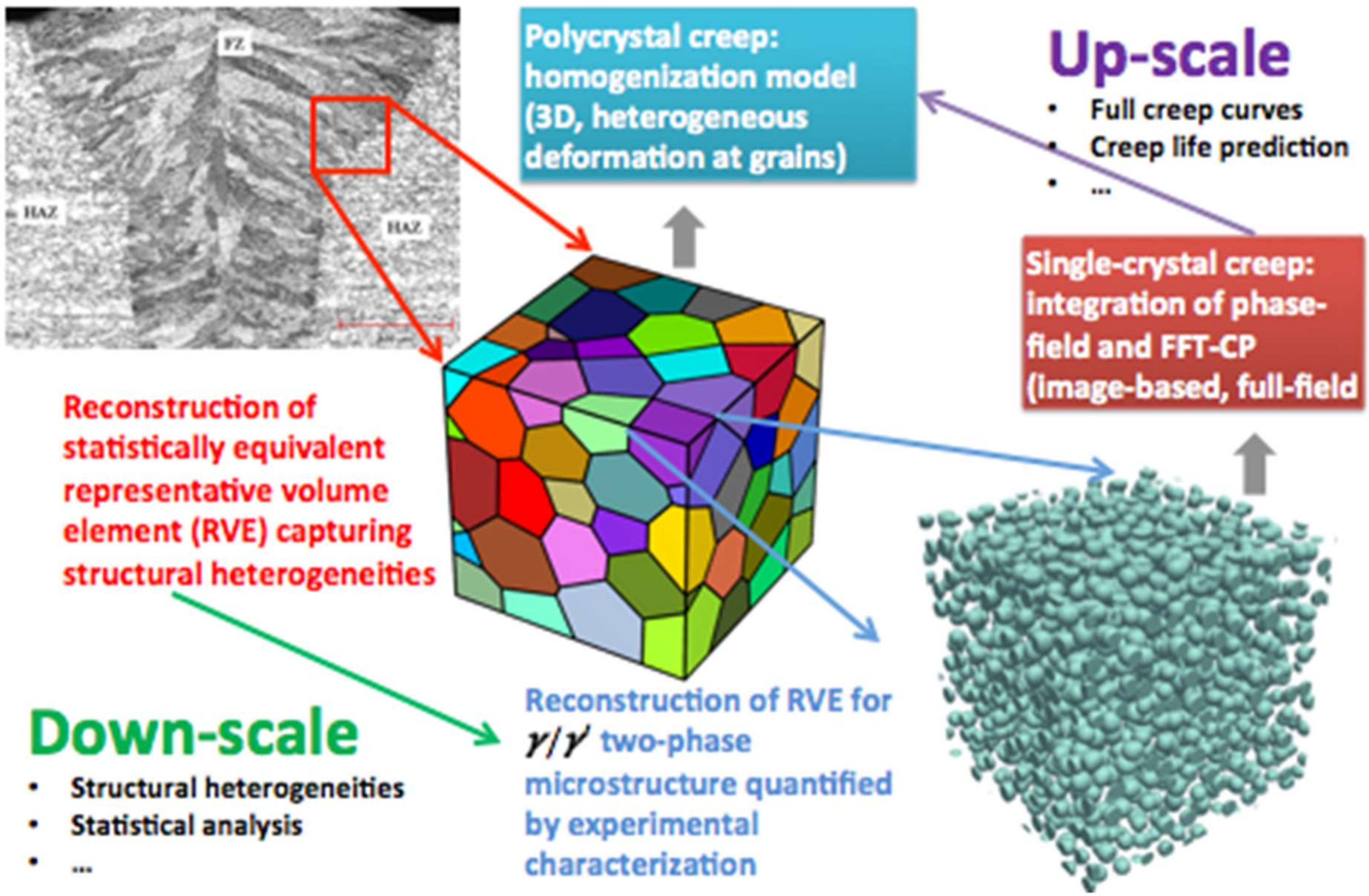

Outline

- Application of machine learning methods for prediction of structure-property relationships in Ni-base superalloys.
  - A fast-acting, reduced-order, data-driven tool

- **Development of a multiscale physics-based creep model for Ni-base superalloys**
  - Integrated creep model at single crystal level
  - Homogenized creep model at polycrystal level

FFT based Micromechanical Solver

Spectral (FFT) method

- Solutions are approximated by *global* Fourier series.
- Stress equilibrium is satisfied at every (image) sampling point in the *strong* form, i.e.,

$$\nabla \cdot \boldsymbol{\sigma} = \mathbf{0}$$

Lebensohn, R. A., et al. (2012). *IJP*.

Finite element method

- Solutions are approximated by *localized* shape-functions
- Stress equilibrium is satisfied in over elements in the *weak* form, i.e.,

$$\int_V \delta\phi \cdot (\nabla \cdot \boldsymbol{\sigma}) dV = \mathbf{0}$$

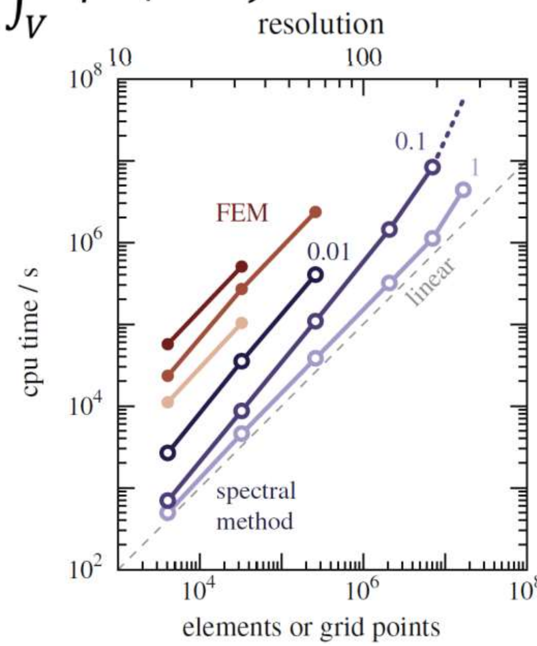

Eisenlohr, P., et al. (2013). *IJP*.

Advantage of FFT method for this study:

- Account for complex geometry of γ/γ' microstructure
- Fast numerical implementation due to FFT algorithm
- Integration with phase-field

Phase-Field Model for γ/γ' Microstructure

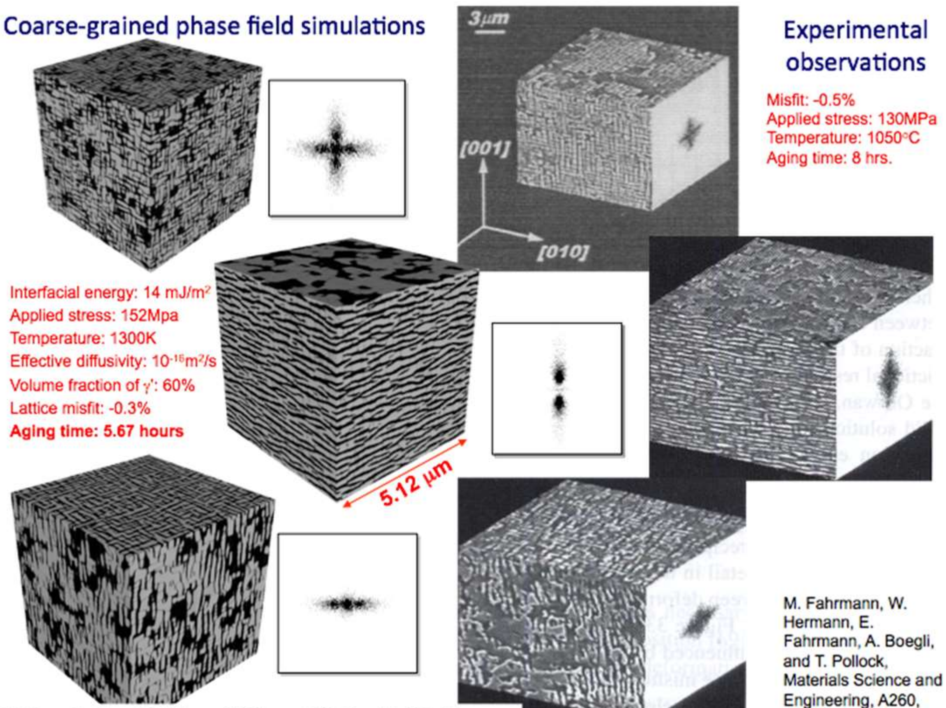

N. Zhou, C. Shen, MJ.Mills and Y. Wang, ***Phil. Mag.*** **90**:405-436 (2010)

M. Fahrmann, W. Hermann, E. Fahrmann, A. Boegli, and T. Pollock, Materials Science and Engineering, A260, 212–221 (1999).

$$F = \int_V \left[f\left(c(\mathbf{x}), \{\phi_i(\mathbf{x})\}_{i=1}^4\right) + \frac{\kappa^2}{2} \sum_{i=1}^{4} (\nabla \phi_i(\mathbf{x}))^2 \right] dV + E^{\text{elast}}$$

$$\frac{\partial c(\mathbf{x})}{\partial t} = \nabla \cdot \left[M \nabla \left(\frac{\delta F}{\delta c(\mathbf{x})} \right) \right]$$

$$\frac{\partial \phi_i(\mathbf{x})}{\partial t} = -L \frac{\delta F}{\delta \phi_i(\mathbf{x})}$$

Improvements

- **C++, MPI parallelization**
- **Incorporate modulus mismatch**

$$\begin{aligned} E^{\text{elast}} &= \frac{1}{2}\int_V \left[C^0_{ijmn}\Delta S_{mnpq}(\mathbf{x})C^0_{pqkl} - C^0_{ijkl}\right]\Delta\epsilon_{ij}(\mathbf{x})\Delta\epsilon_{kl}(\mathbf{x})dV \\ &+ \frac{1}{2}\int_V C^0_{ijkl}[\epsilon_{ij}(\mathbf{x}) + \Delta\epsilon_{ij}(\mathbf{x})][\epsilon_{kl}(\mathbf{x}) + \Delta\epsilon_{kl}(\mathbf{x})]dV - \bar{\varepsilon}_{ij}\int_V C^0_{ijkl}[\epsilon_{kl}(\mathbf{x}) + \Delta\epsilon_{kl}(\mathbf{x})]dV \\ &+ \frac{V}{2}C^0_{ijkl}\bar{\varepsilon}_{ij}\bar{\varepsilon}_{kl} - \frac{1}{2}\fint \frac{d^3k}{(2\pi)^3}[\tilde{\sigma}_{ij}(\mathbf{k}) + \Delta\tilde{\sigma}_{ij}(\mathbf{k})]\Gamma_{jikl}(\mathbf{n})[\tilde{\sigma}_{kl}(\mathbf{k}) + \Delta\tilde{\sigma}_{kl}(\mathbf{k})]^* \end{aligned}$$

$$\begin{aligned} \frac{\delta E^{\text{elast}}}{\delta\phi_i} &= \frac{1}{2}C^0_{ijmn}\frac{d\Delta S_{mnpq}(\mathbf{x})}{d\phi_i}C^0_{pqkl}\Delta\epsilon_{ij}(\mathbf{x})\Delta\epsilon_{kl}(\mathbf{x}) \\ &+ \left[C^0_{ijmn}\Delta S_{mnpq}(\mathbf{x})C^0_{pqkl} - C^0_{ijkl}\right]\frac{d\Delta\epsilon_{ij}(\mathbf{x})}{d\phi_i}\Delta\epsilon_{kl}(\mathbf{x}) \\ &+ \left(\frac{d\epsilon_{ij}(\mathbf{x})}{d\phi_i} + \frac{d\Delta\epsilon_{ij}(\mathbf{x})}{d\phi_i}\right)\left[C^0_{ijkl}\epsilon^0_{kl}(\mathbf{x}) - C^0_{ijkl}\bar{\epsilon}^0_{kl} - \left\langle C^0_{mnij}\Gamma_{mnkl}(\mathbf{n})C^0_{klts}\tilde{\epsilon}^0_{ts}(\mathbf{k})\right\rangle_{\mathbf{x}} - \sigma^{\text{appl}}_{ij}\right] \end{aligned}$$

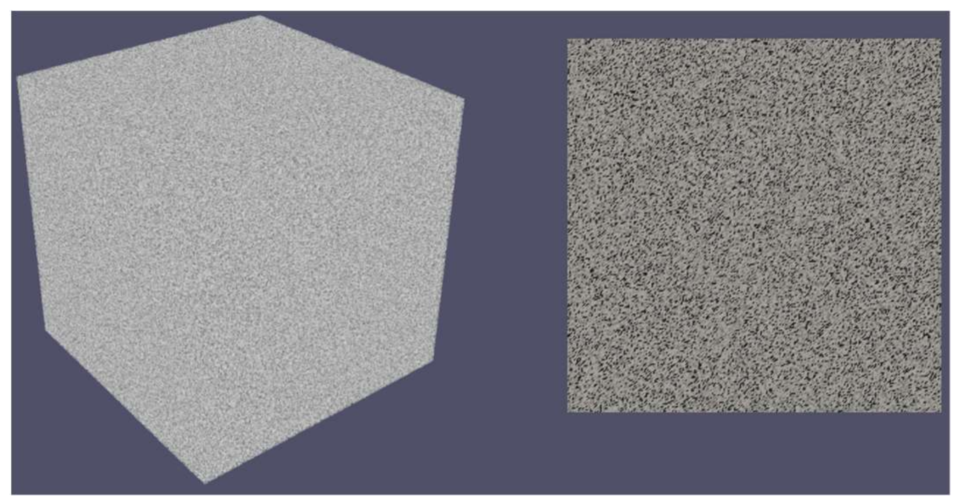

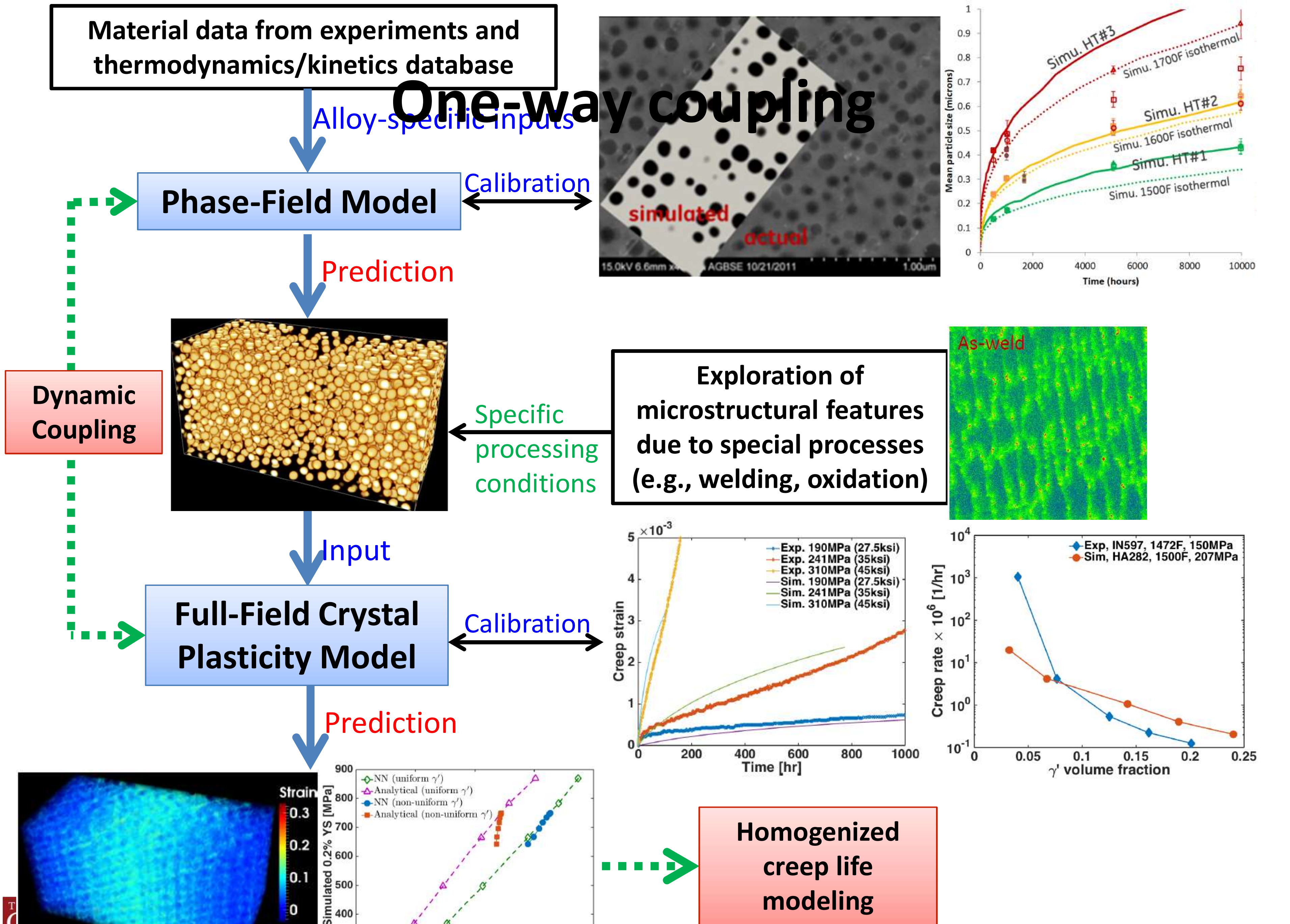

NETL Award No. DE-FE0024027

Dynamic coupling of phase-field and FFT-CP

Elastic strain
- Satisfy the stress-equilibrium equation

Transformation strain (microstructure)
- Use LROs and composition fields to describe the evolution

Plastic strain (plasticity)
- Use dislocation density fields to describe the evolution

$$\varepsilon_{ij}(\mathbf{x}) = e_{ij}(\mathbf{x}) + \epsilon^{\mathrm{t}}_{ij}(\mathbf{x}) + \epsilon^{\mathrm{p}}_{ij}(\mathbf{x})$$

Cottura, M., et al. *JMPS,* 94 (2016): 473.

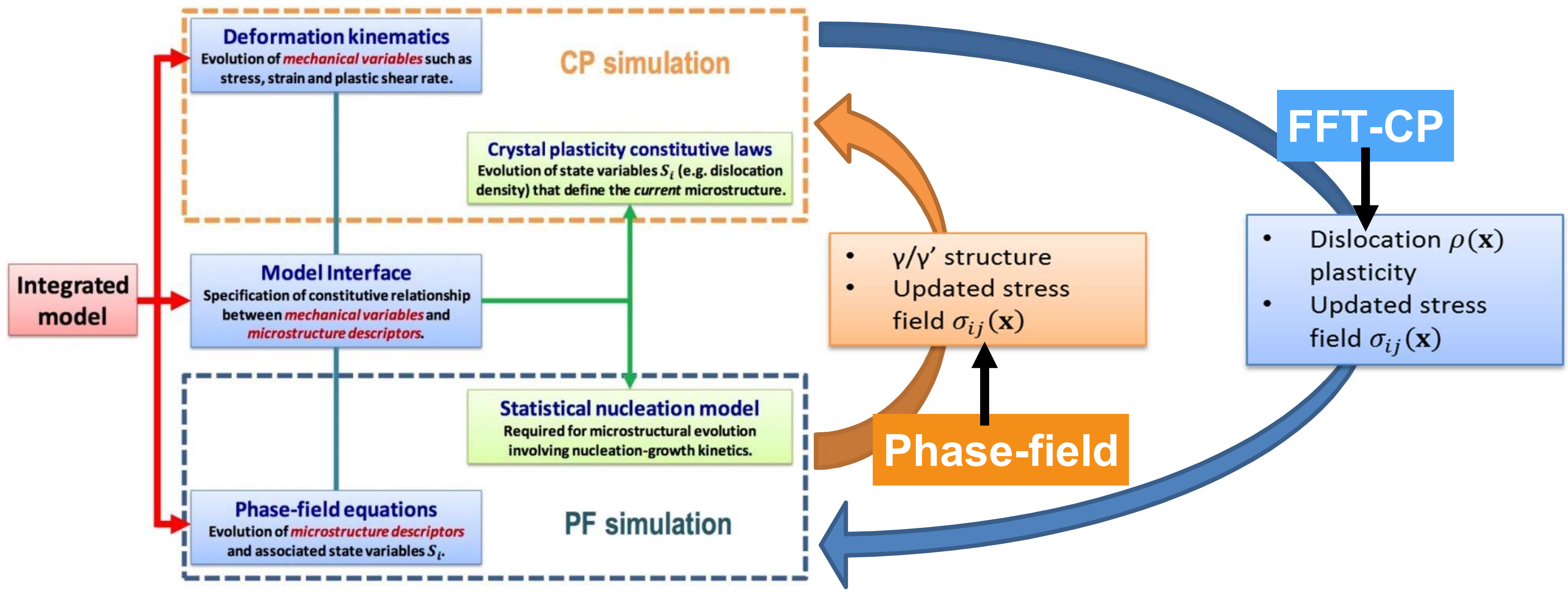

Zhao, Low, Wang, and Niezgoda IJP, 80(2016): 38

Prediction: γ’ Evolution Accelerates Creep

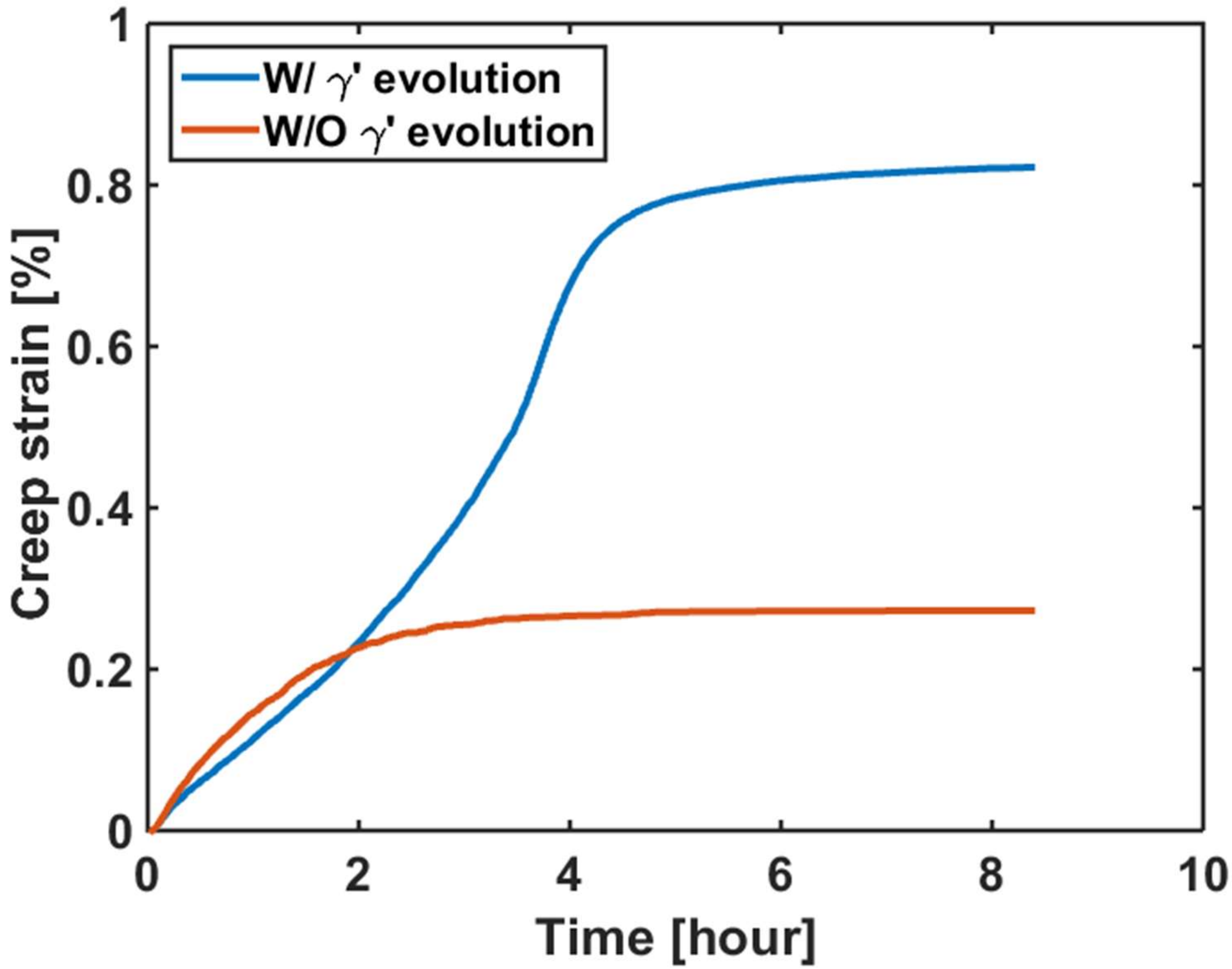

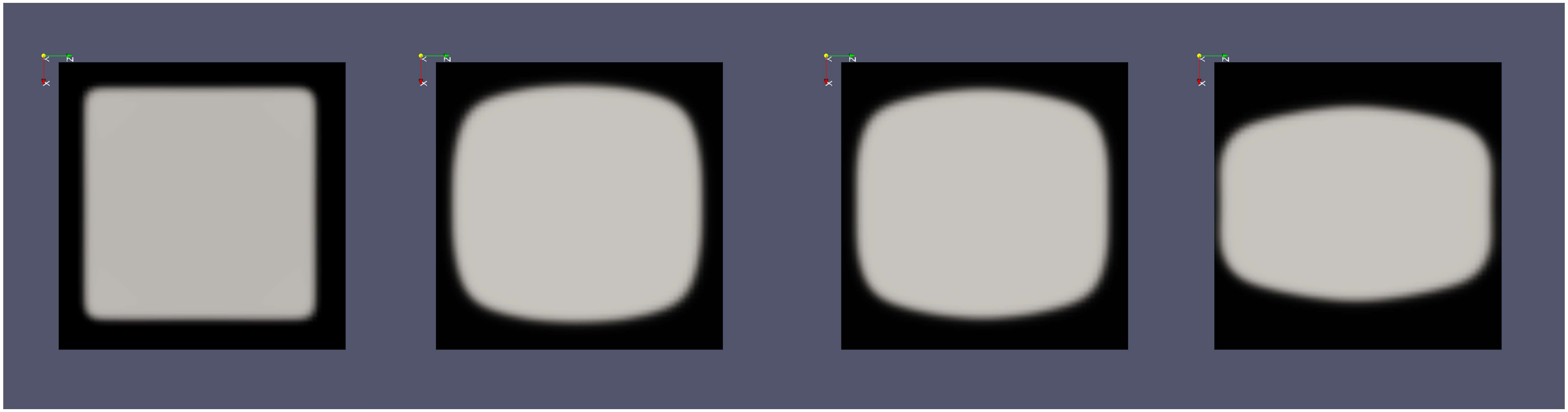

The interplay between plasticity and microstructure:

- The γ’ directional coarsening eliminates the vertical channels and widen the horizontal channels.
- The increase of horizontal channel volume fraction accelerates dislocation glide, leading to the experimentally observed high primary creep rate.

Prediction: Plasticity Stabilizes Wavy Interface

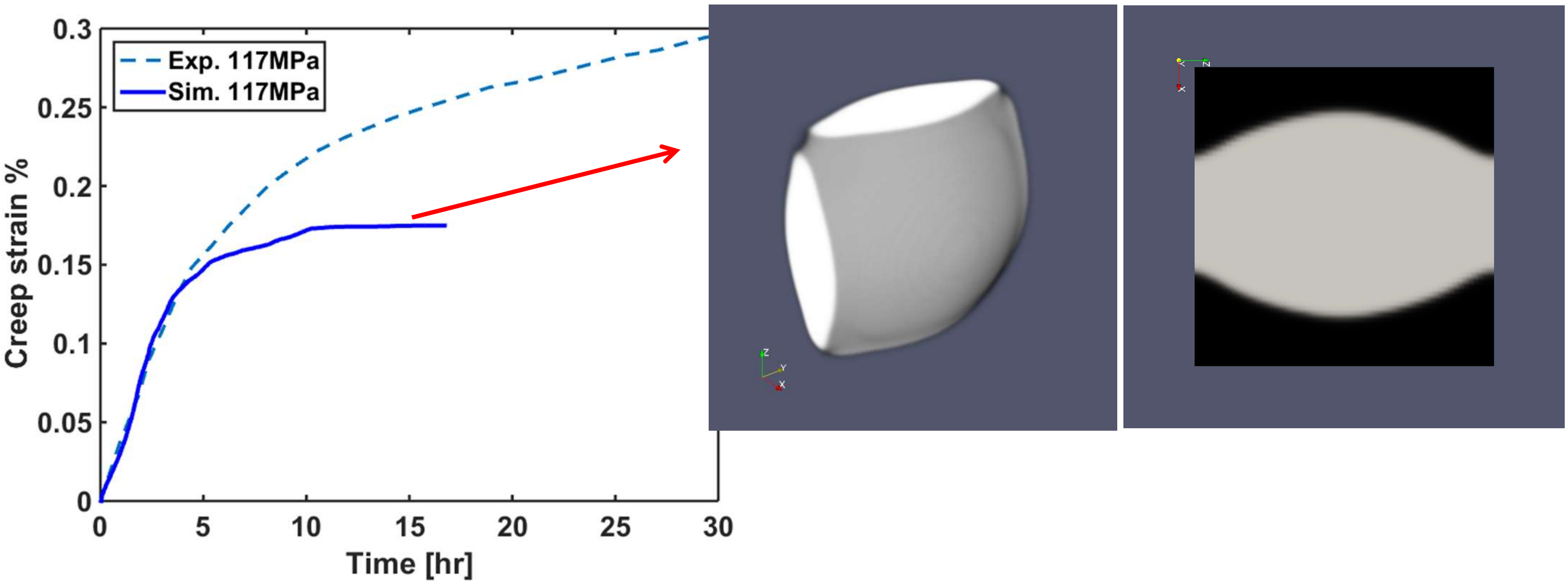

Prediction: Plasticity Stabilizes Wavy Interface

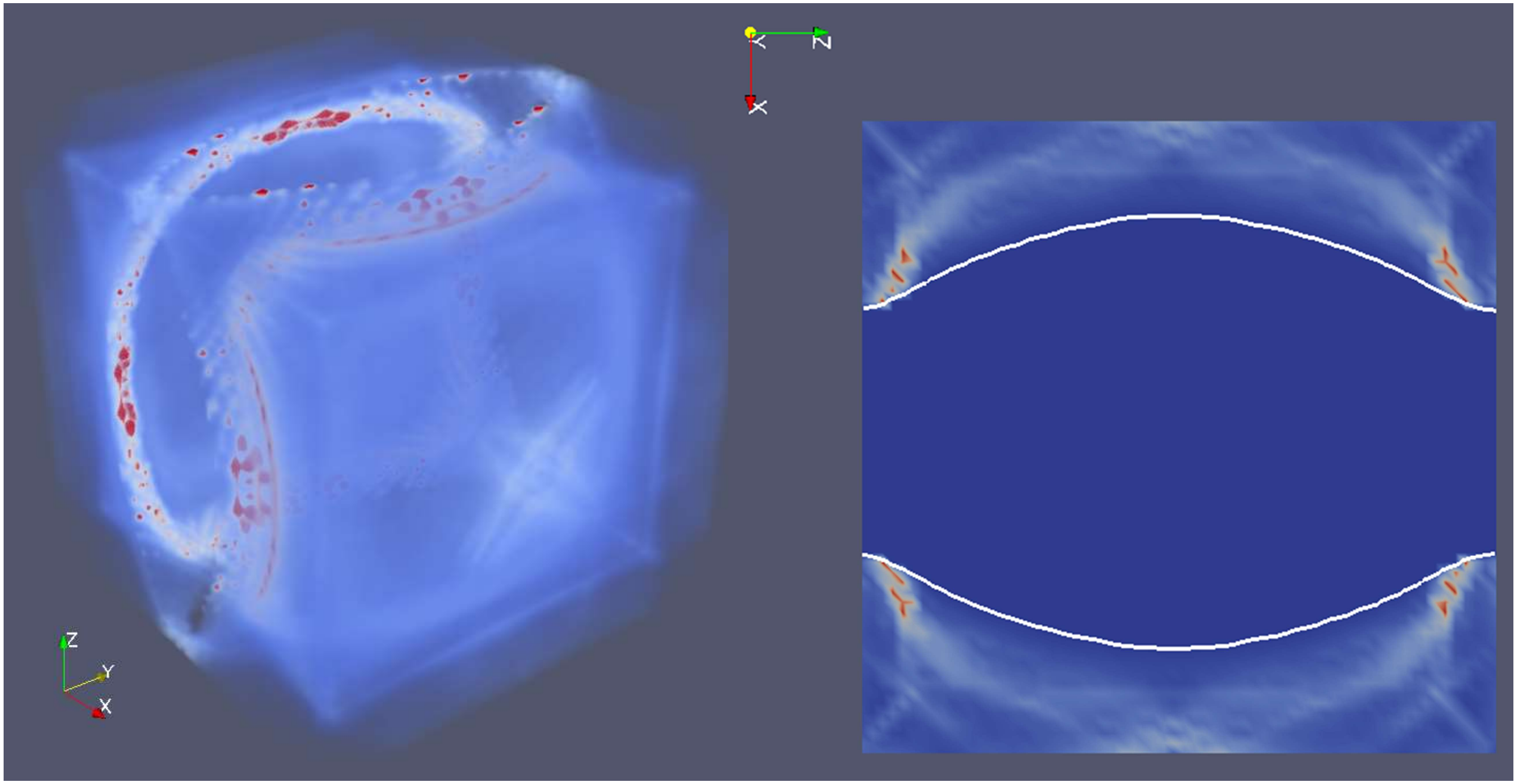

Geometrically necessary dislocation (GND) density

Prediction: Plasticity Stabilizes Wavy Interface

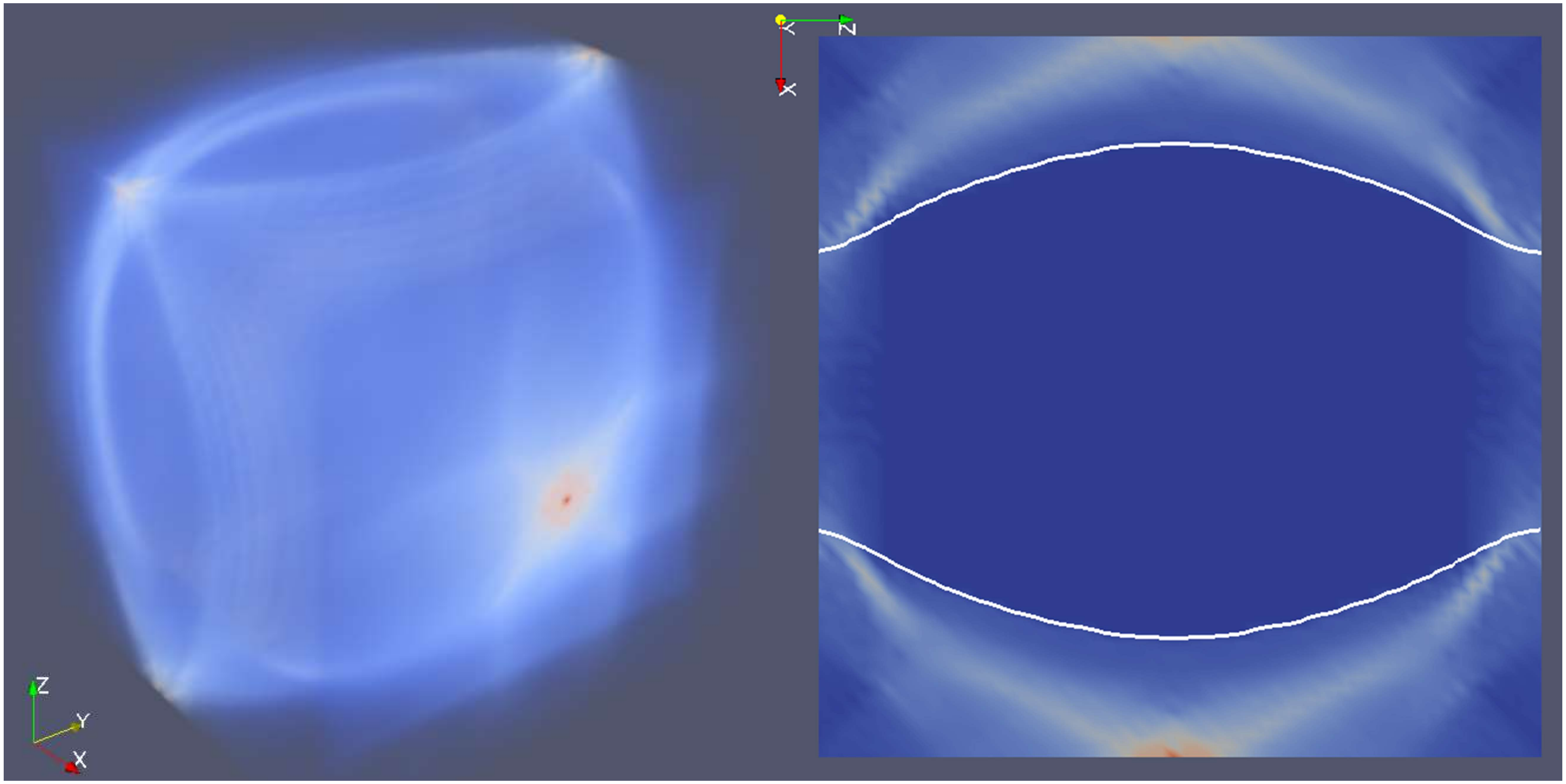

Plastic strain distribution

Wavy γ/γ' Interface in Experiments

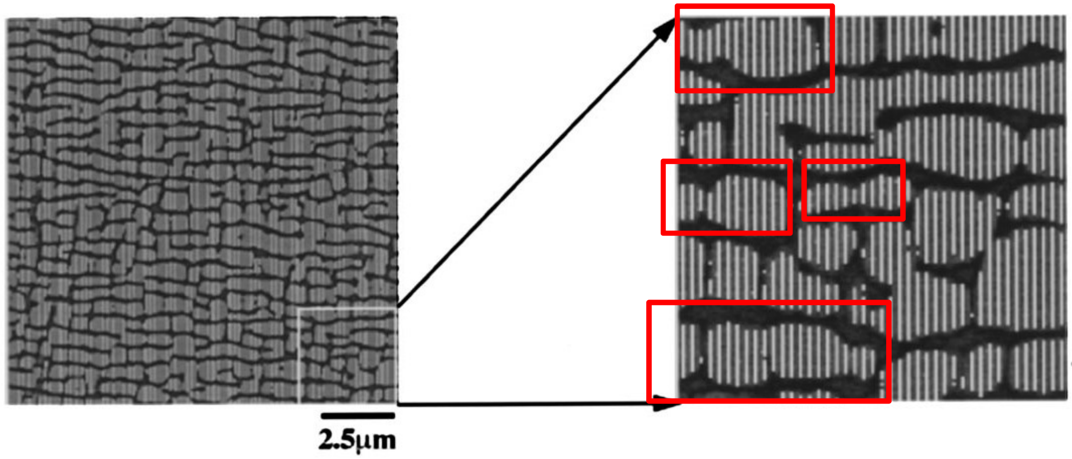

CMSX-4, 0.27% creep strain (Matan, Reed, et al, 1999)

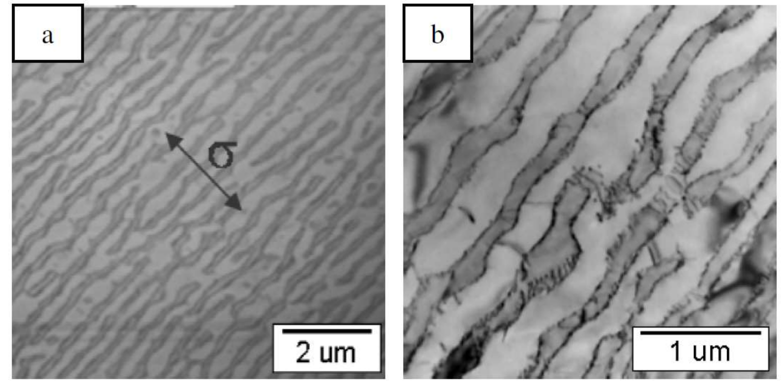

PWA1484, 1.0% creep strain (Czyrska-Filemonowicz, et al, 2007)

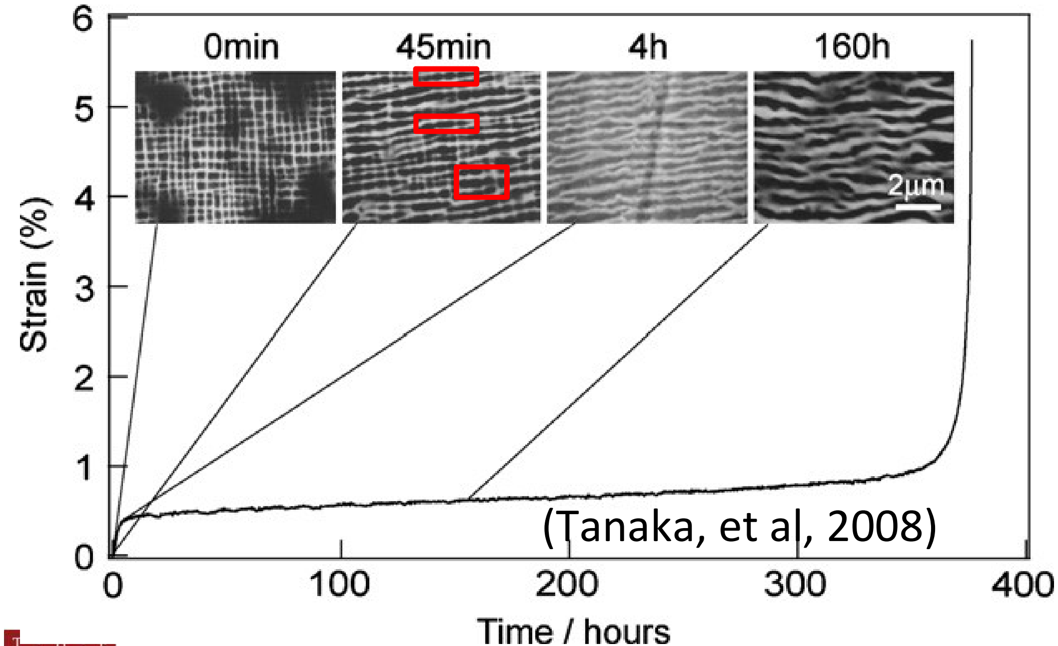

(Tanaka, et al, 2008)

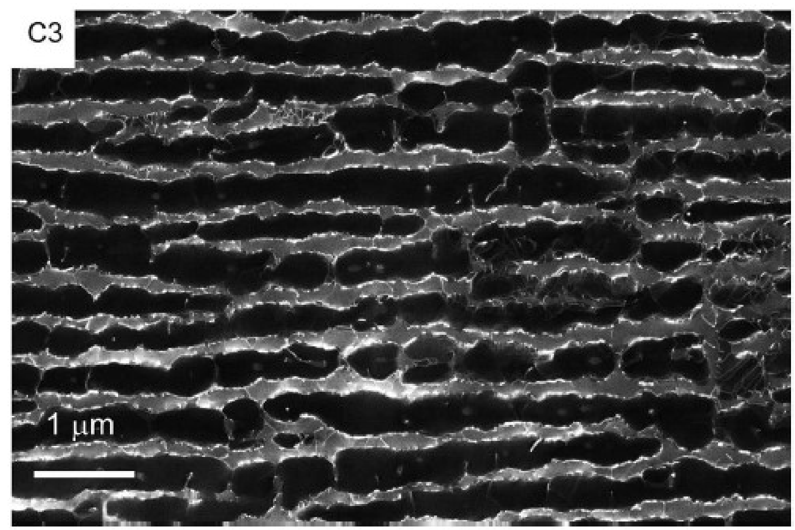

(Ram, et al, 2016)

μ^{diff} from Simulations

W/O plasticity

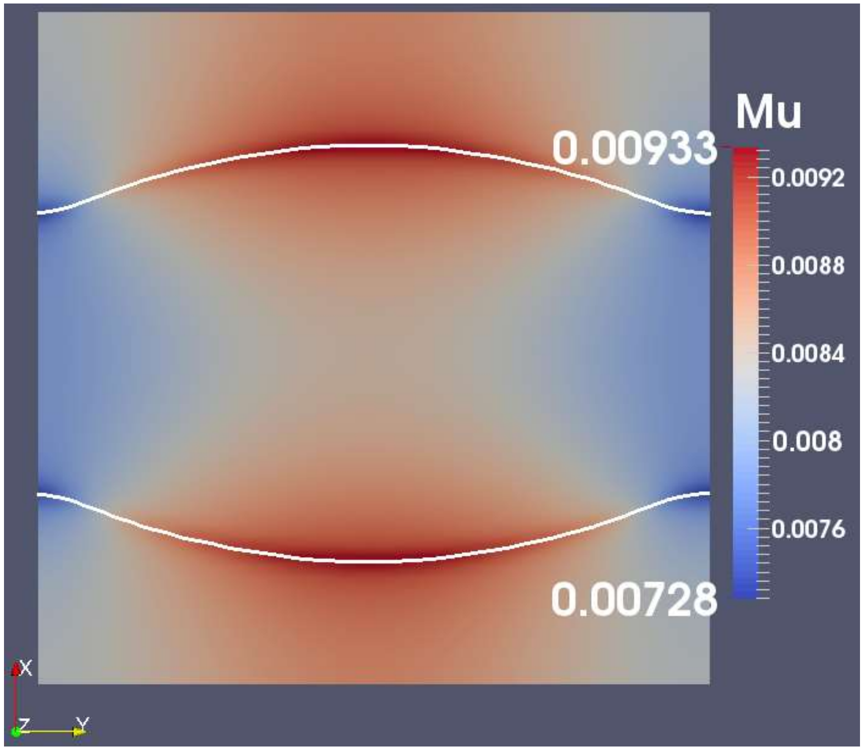

W/ plasticity

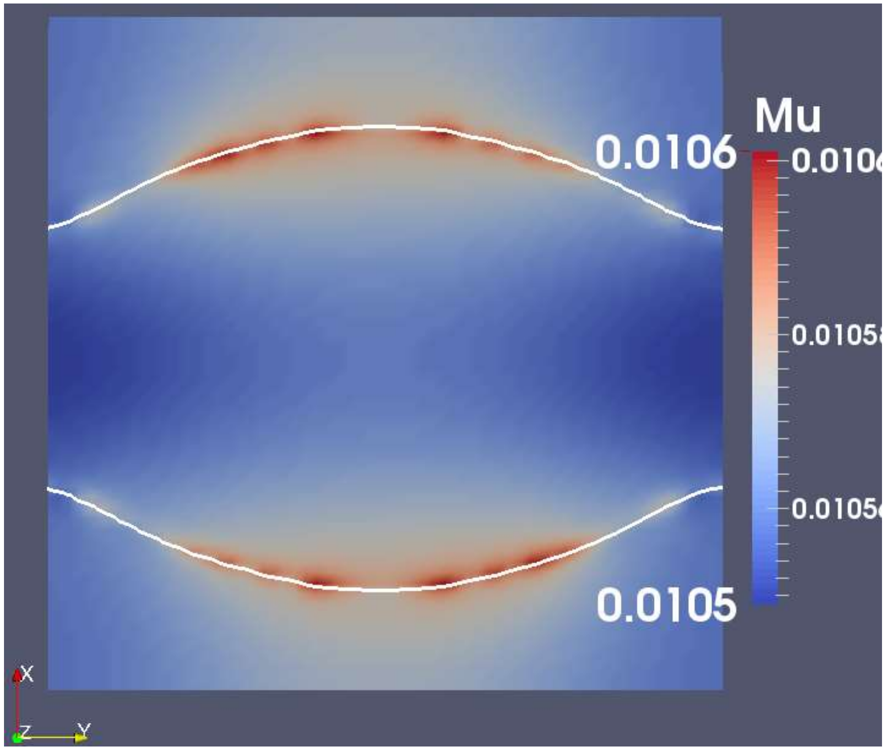

$$\frac{\max(\mu^{\text{diff}}) - \min(\mu^{\text{diff}})}{\min(\mu^{\text{diff}})} = 28.2\%$$

$$\frac{\max(\mu^{\text{diff}}) - \min(\mu^{\text{diff}})}{\min(\mu^{\text{diff}})} = 1.0\%$$

Prediction: Plasticity Stabilizes Small γ’

Static (W/O stress)

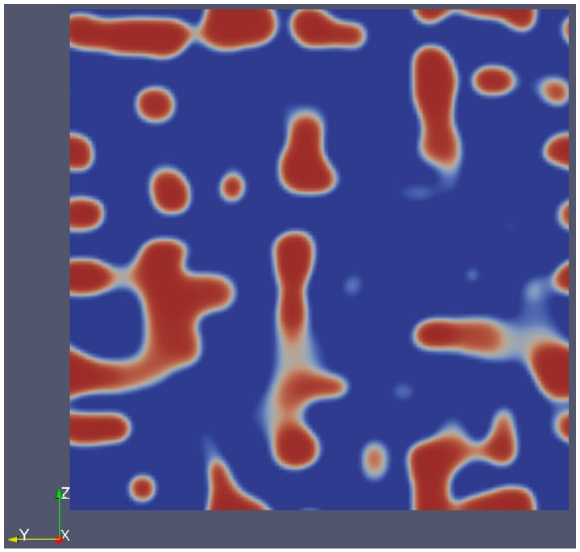

Stress (W/O plasticity)

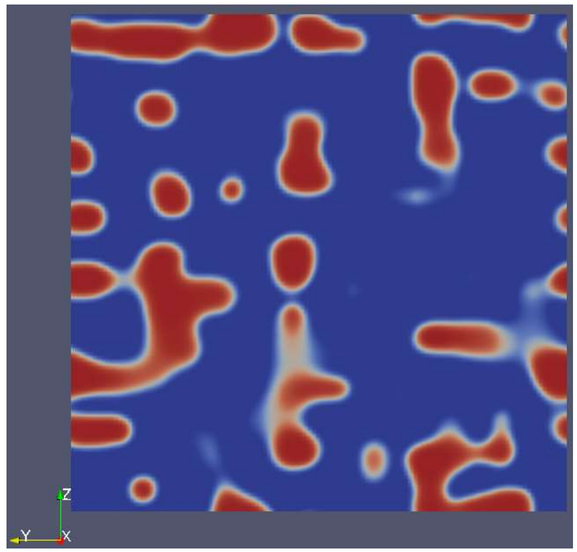

Stress (W/ plasticity)

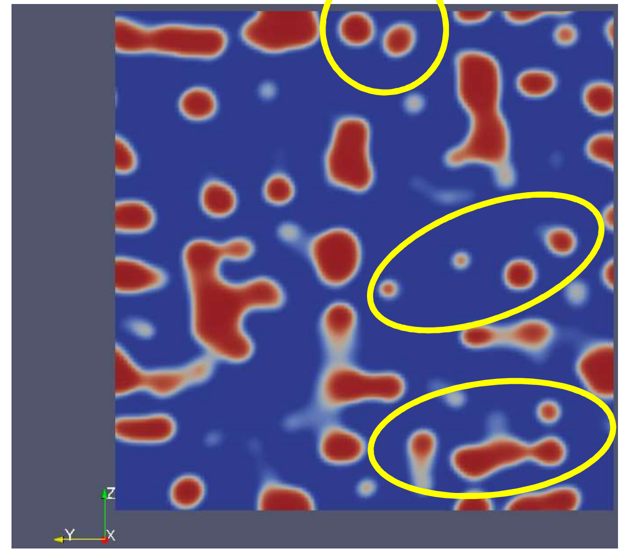

- **The number of γ’ particles for stress W/ plasticity is apparently larger than the other two cases.**

Experiments on H282

Intragranular γ′ Evolution: Static Exposure vs Creep

Creep

1500F/25ksi/1606hrs

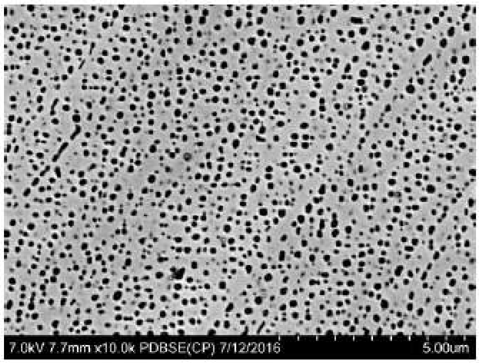

1600F/15ksi/1678hrs

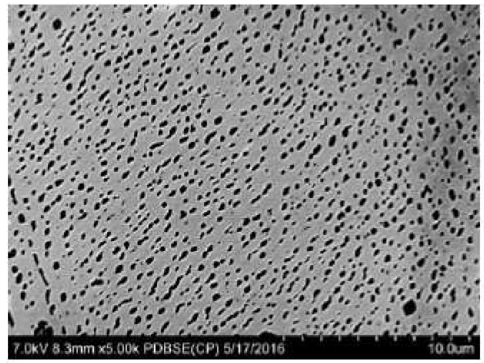

1700F/8ksi/1000hrs

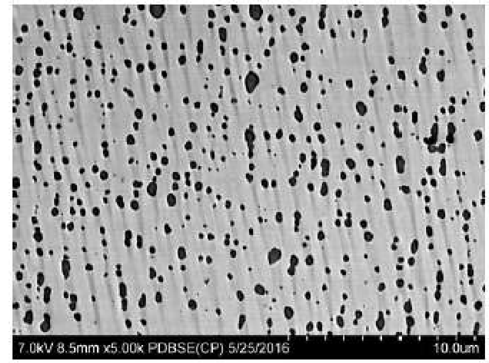

Static Exposure

1500F, 1000hrs

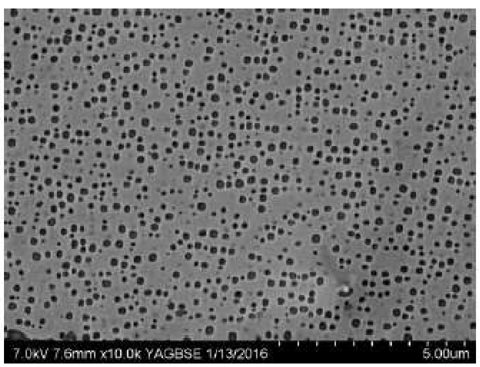

1600F, 1000hrs

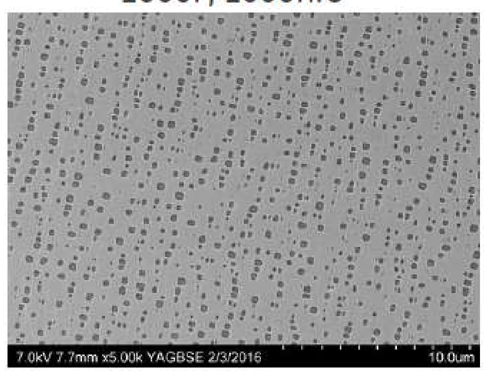

1700F, 1000hrs

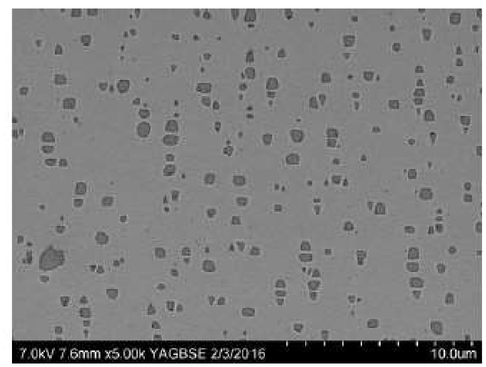

Courtesy of Chen Shen

Prediction: Plasticity Leads Smaller Mean γ' Size

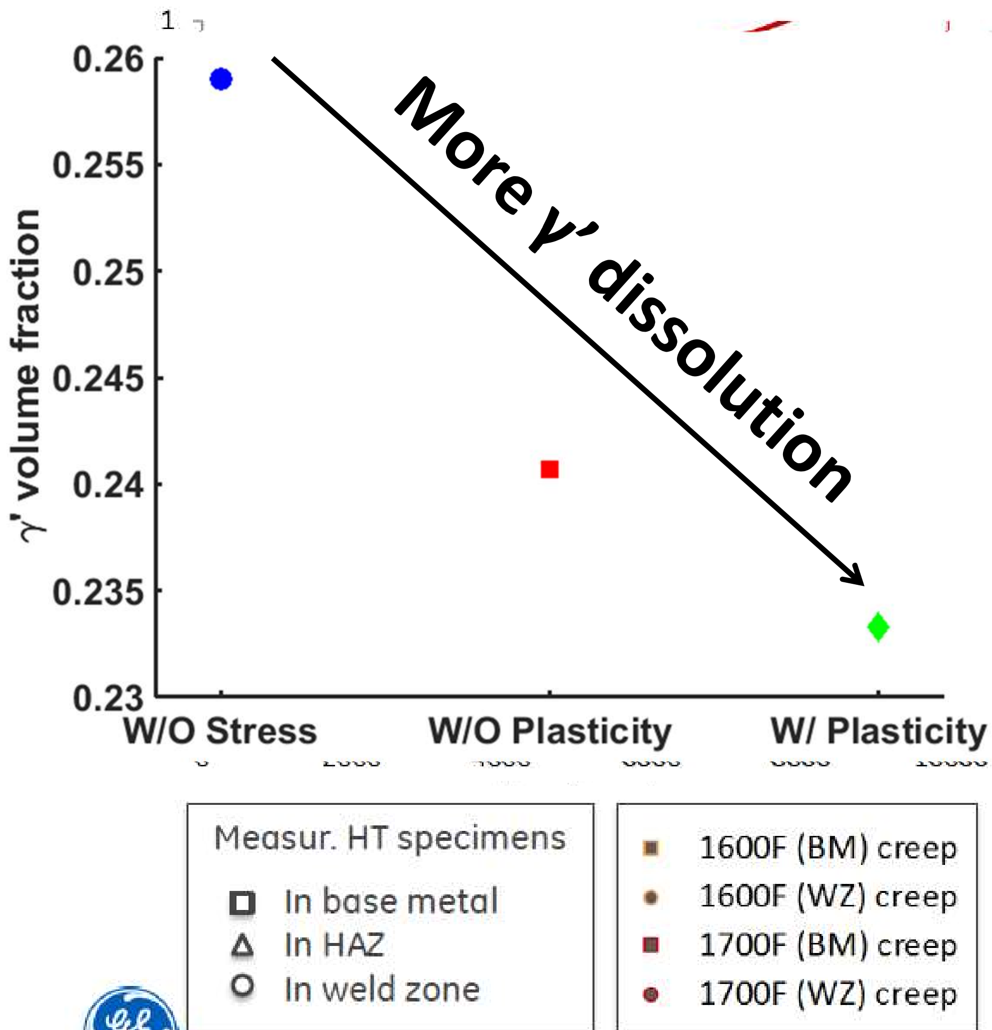

Courtesy of Chen Shen

- **Adding plasticity promotes more dissolution of γ'**
- **Combined with the increased number density due to plasticity, the average γ' size is expected to be smaller than that during static exposure.**

Outline

- Application of machine learning methods for prediction of structure-property relationships in Ni-base superalloys.

  A fast-acting, reduced-order, data-driven tool

- **Development of a multiscale physics-based creep model for Ni-base superalloys**

  Integrated creep model at single crystal level

  Homogenized creep model at polycrystal level

Homogenized Polycrystalline Creep Model

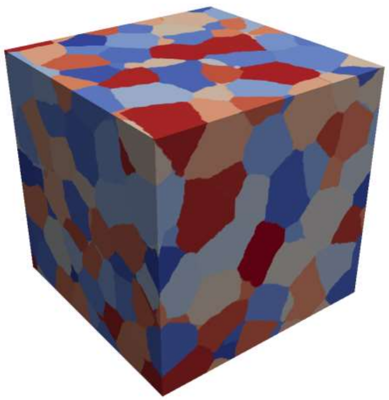

191 grains

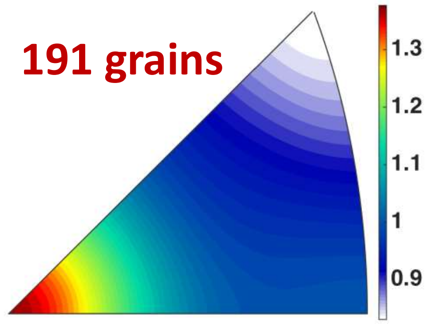

Synthetic grain structure from DREAM3D

Experimental characterization + 3D microstructure reconstruction

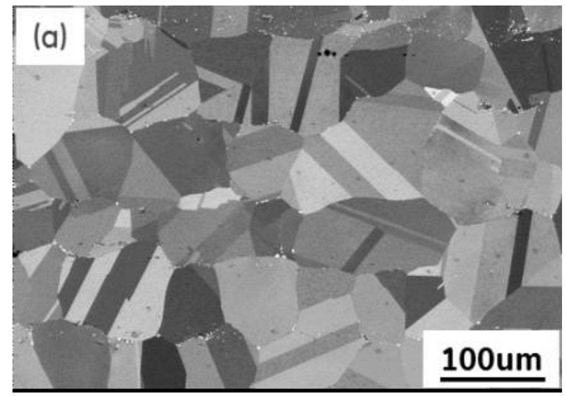

H282, Chen, et. al., 2017

Extended Voce hardening (Tome, et al, 1984)

Kocks-Mecking model + Taylor hardening

$$\dot{\rho} = \left(k_1\sqrt{\rho} - k_2\rho\right)\dot{\Gamma}$$

$$\tau = \tau_0 + \alpha\mu b\sqrt{\rho}$$

$$\boxed{\hat{\tau}^s = \tau_0^s + (\tau_1^s + \theta_1^s\Gamma)(1 - \exp(-\Gamma\left|\frac{\theta_0^s}{\tau_1^s}\right|))}$$

Five fitting parameters: $\tau_0, \tau_1, \theta_0, \theta_1, \dot{\gamma}_0$

$$\boxed{\dot{\varepsilon}_{ij} = \dot{\gamma}_0 \sum_s m_{ij}^s \left(\frac{m_{kl}^s \sigma_{kl}}{\tau^s}\right)^n}$$

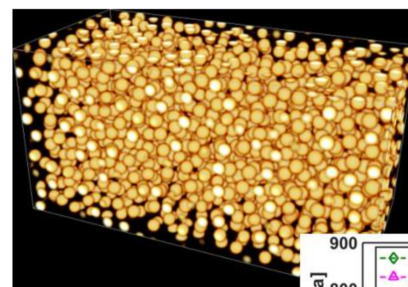

Single grain modeling

Predicted structure-property relation at γ/γ' level

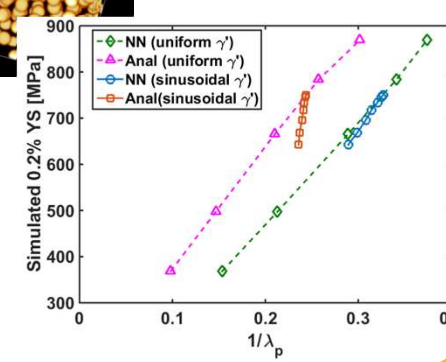

Homogenized simulations of H282 tensile tests

Dislocation model at γ/γ’ microstructure level

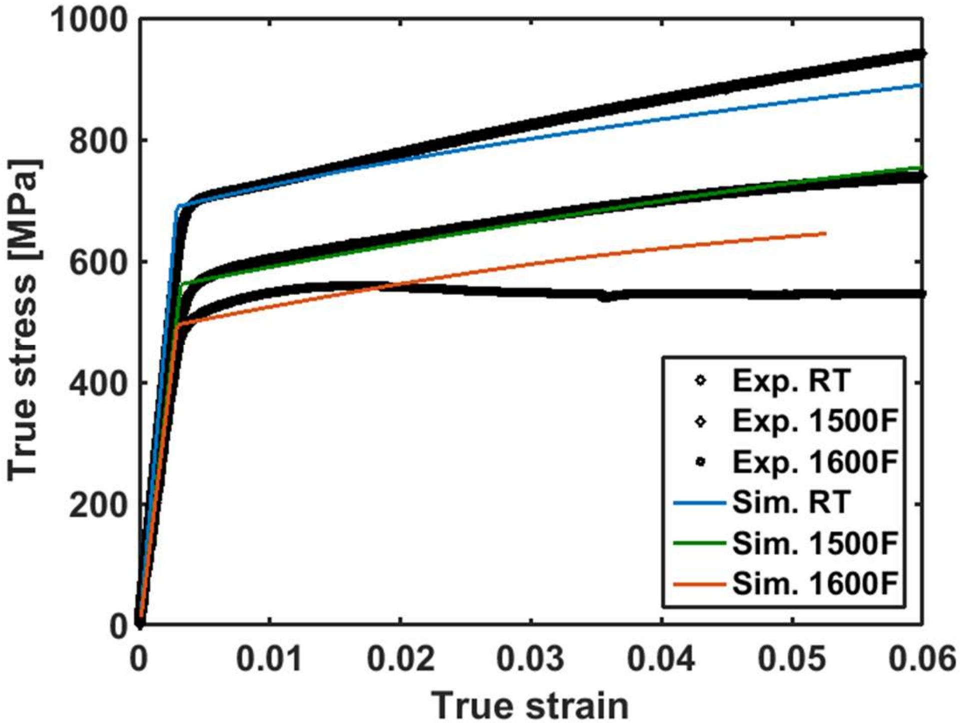

Homogenized model at polycrystal level

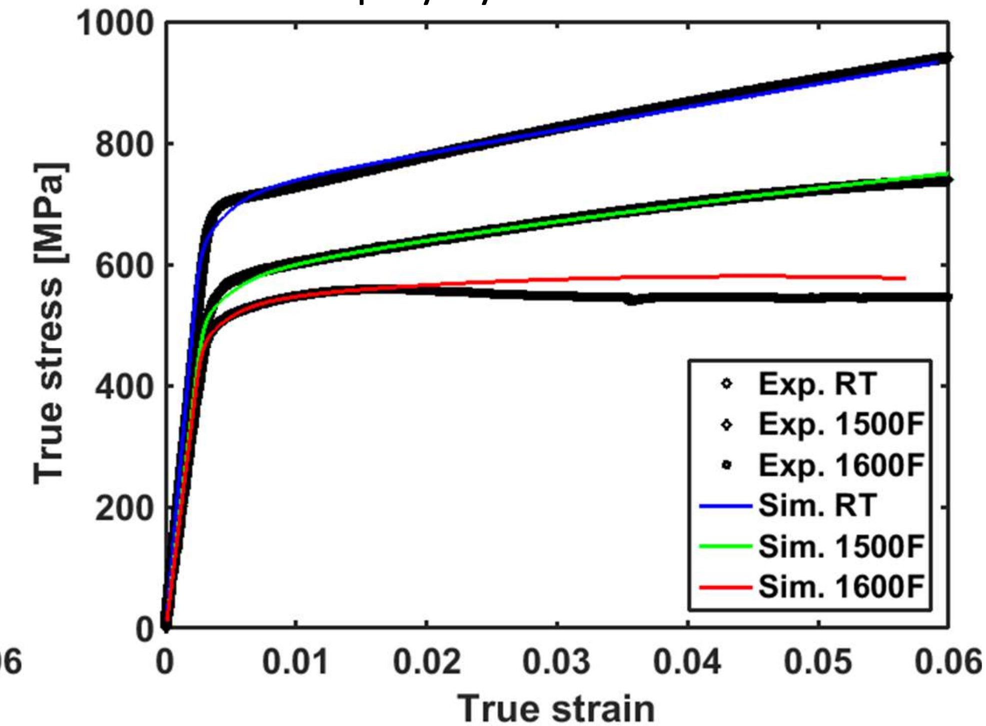

- **The temperature-dependence of Voce hardening parameters can be further justified physically based on single-grain dislocation-based simulation predictions.**
- **Surprisingly the apparent softening can be captured by the current Voce hardening.**

Micromechanical Fields in Tensile Tests

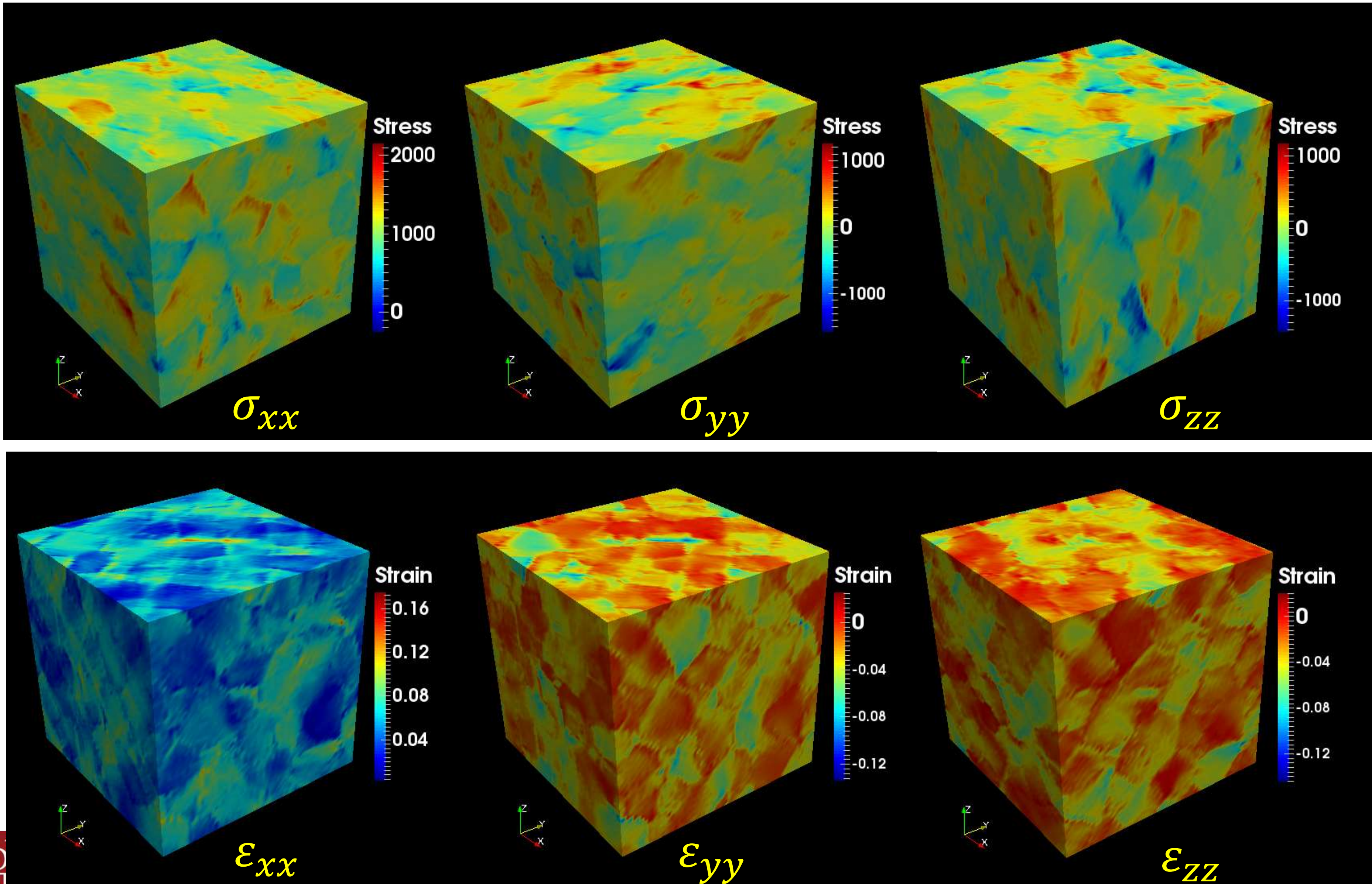

Homogenized simulations of H282 creep

Dislocation model at γ/γ' microstructure level

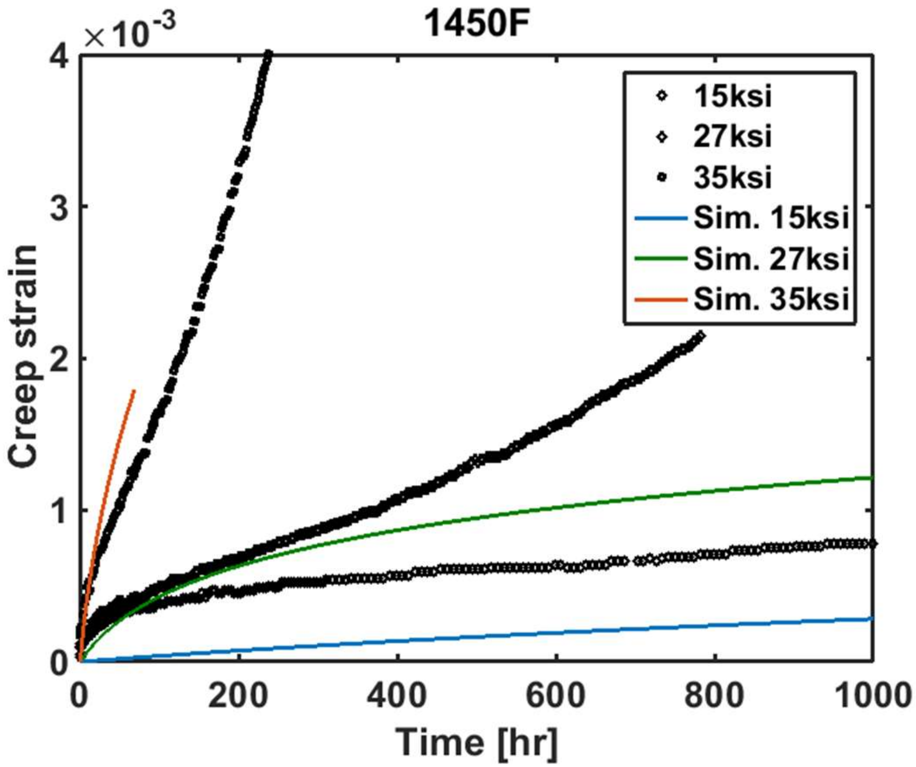

Homogenized model at polycrystal level

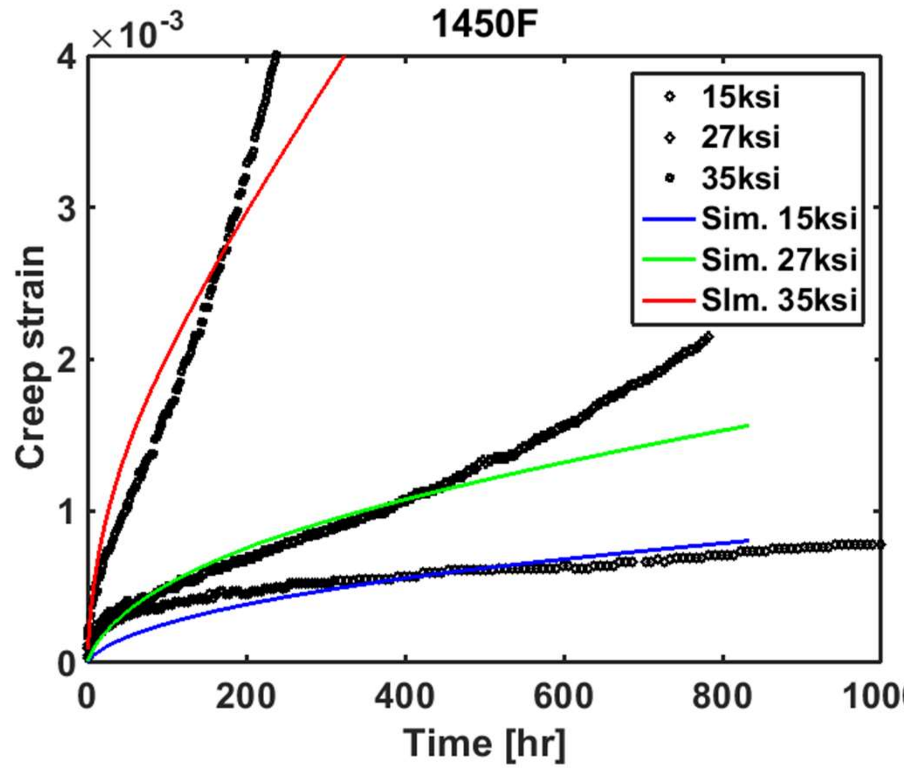

- **The failure of capturing low-stress creep behavior using dislocation model can be overcome by the homogenized model.**
- **The only stress-dependent parameter is $\dot{\gamma}_0$, which may be further rationalized based on physical arguments/simulations.**

Micromechanical Fields in Creep Tests

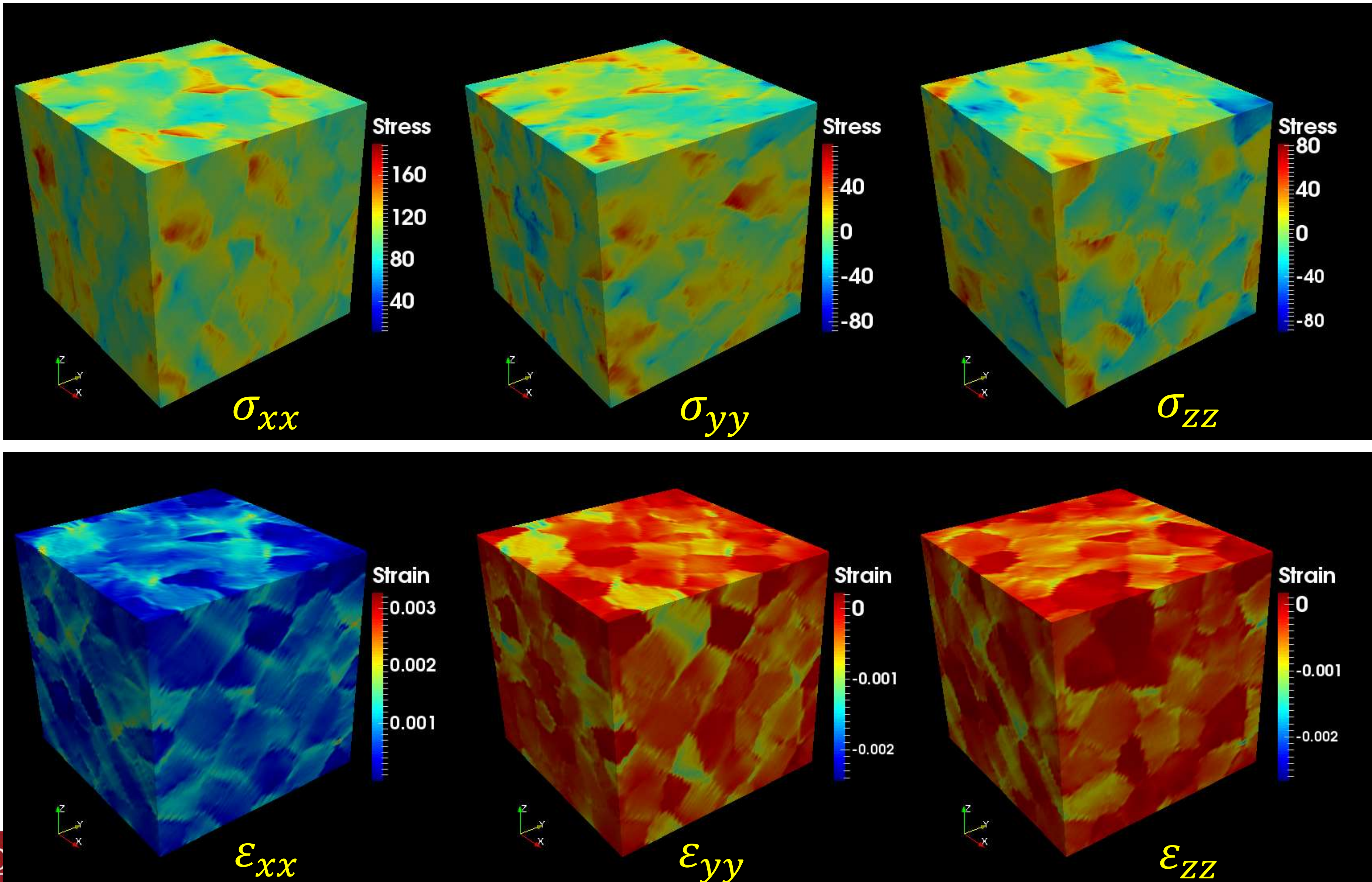

Summary & Future Work

- **A fast-acting, reduced-order, data-driven tool has been developed, verified, and validated using VPSC generated data**
  - ➢ Application to existing experimental data and creep life models
- **Creep models of Ni-base superalloys have been developed at both single crystal and polycrystal levels**
  - ➢ Application to long-term creep life prediction
  - ➢ Effects of structural heterogeneities on creep